

Article

Estimation of Knee Joint Extension Force Using Mechanomyography Based on IGWO-SVR Algorithm

Zebin Li ^{1,2,3,*} , Lifu Gao ¹, Wei Lu ^{1,2}, Daqing Wang ¹ , Chenlei Xie ¹ and Huibin Cao ^{1,*}

¹ Institute of Intelligent Machines, Hefei Institutes of Physical Science, Chinese Academy of Sciences, Hefei 230031, China; lifugao@iim.ac.cn (L.G.); lw9296@mail.ustc.edu.cn (W.L.); dqwang@mail.ustc.edu.cn (D.W.); xiecl@mail.ustc.edu.cn (C.X.)

² Department of Science Island, University of Science and Technology of China, Hefei 230026, China

³ School of Electrical and Photoelectric Engineering, West Anhui University, Lu'an 237012, China

* Correspondence: robotzebinli@foxmail.com (Z.L.); hbcao@iim.ac.cn (H.C.)

Abstract: Muscle force is an important physiological parameter of the human body. Accurate estimation of the muscle force can improve the stability and flexibility of lower limb joint auxiliary equipment. Nevertheless, the existing force estimation methods can neither satisfy the accuracy requirement nor ensure the validity of estimation results. It is a very challenging task that needs to be solved. Among many optimization algorithms, gray wolf optimization (GWO) is widely used to find the optimal parameters of the regression model because of its superior optimization ability. Due to the traditional GWO being prone to fall into local optimum, a new nonlinear convergence factor and a new position update strategy are employed to balance local and global search capability. In this paper, an improved gray wolf optimization (IGWO) algorithm to optimize the support vector regression (SVR) is developed to estimate knee joint extension force accurately and timely. Firstly, mechanomyography (MMG) of the lower limb is measured by acceleration sensors during leg isometric muscle contractions extension training. Secondly, root mean square (RMS), mean absolute value (MAV), zero crossing (ZC), mean power frequency (MPF), and sample entropy (SE) of the MMG are extracted to construct feature sets as candidate data sets for regression analysis. Lastly, the features are fed into IGWO-SVR for further training. Experiments demonstrate that the IGWO-SVR provides the best performance indexes in the estimation of knee joint extension force in terms of RMSE, MAPE, and R compared with the other state-of-art models. These results are expected to become the most effective as guidance for rehabilitation training, muscle disease diagnosis, and health evaluation.

Keywords: mechanomyography; knee joint extension force; improved gray wolf algorithm; support vector machine



check for updates

Citation: Li, Z.; Gao, L.; Lu, W.; Wang, D.; Xie, C.; Cao, H. Estimation of Knee Joint Extension Force Using Mechanomyography Based on IGWO-SVR Algorithm. *Electronics* **2021**, *10*, 2972. <https://doi.org/10.3390/electronics10232972>

Academic Editors: YangQuan Chen, Subhas Mukhopadhyay, Nunzio Cennamo, Mohamed Jamal Deen, Junseop Lee, Simone Morais and Jichai Jeong

Received: 1 October 2021

Accepted: 25 November 2021

Published: 29 November 2021

Publisher's Note: MDPI stays neutral with regard to jurisdictional claims in published maps and institutional affiliations.



Copyright: © 2021 by the authors. Licensee MDPI, Basel, Switzerland. This article is an open access article distributed under the terms and conditions of the Creative Commons Attribution (CC BY) license (<https://creativecommons.org/licenses/by/4.0/>).

1. Introduction

With the rapid increase in global aging, the elderly are more likely to lose their ability to exercise due to stroke, arthritis, central nervous system diseases, and other diseases. According to the Indian Aging Report 2017, the cases of arthritis and stroke among the elderly may increase up to 55.9 million and 1.9 million, respectively, by 2030 [1]. In addition, millions of people around the world have lost limbs for various reasons, and according to the World Health Organization, there are approximately 40 million amputees in the world [2,3]. High-performance prosthetics and rehabilitation training equipment can significantly improve the quality of life of the elderly and patients with lost limbs. However, at present, the product gap of assistive devices is huge, and the intelligence degree is not high. Simple manual supervision or simple assistive devices have been unable to meet the needs of the disabled and the elderly. Therefore, safe and reliable auxiliary training instruments and intelligent and convenient prosthetic devices will greatly improve

the daily living standards of these groups, which has also attracted extensive attention from robotics researchers [4].

Auxiliary training instruments and intelligent prosthetic devices need to realize comfortable, natural, and flexible human-machine interaction and human-machine coordinated movement. The key technology lies in the simple, real-time, and accurate acquisition of human motion intentions and parameters related to human dynamics through biological signals on the surface of the human skin [5,6]. In particular, joint extension force estimation is an effective way to improve the flexibility of human joint auxiliary training equipment.

There are usually two methods to obtain the biological signal, namely invasive way and non-invasive way. The non-invasive method has almost no damage to the human body, which has attracted wide attention and shows great application prospects. In general, non-invasive methods such as surface electromyography (sEMG), electroencephalogram (EEG), and mechanomyography (MMG) are used to obtain signals from the human surface. Although sEMG and EEG have been successfully applied in human motion recognition and parameter estimation, these biological signals are easily affected by the external environment, which leads to the instability of the actual signal and brings difficulties to practical application. Specifically, sEMG acquisition usually requires skin preparation and is susceptible to skin impedance, sweating [7]. EEG acquisition usually requires a quiet place to preserve concentration and is susceptible to swallowing, accidental blinking [2]. Studies have shown that during muscle activity, not only sEMG signals are generated, but also low-frequency mechanical vibration signals (MMG) are generated by muscle contraction [8]. MMG records the mechanical phenomenon of transverse vibration of muscles during active contraction and reflects the mechanical properties of muscles in the process of movement [9], which has attracted the attention of some scholars in recent years. Compared with sEMG and EEG, MMG measurements are more reliable because they do not require skin preparation, precise positioning of test positions, and avoidance of accidental body movements. In addition, MMG can be easily detected by general sensors such as accelerometers, piezoelectric contact sensors, and microphones [10] and have stronger anti-interference than sEMG and EEG signals. Moreover, the sensor requirements are lower for MMG signal acquisition [11].

At present, muscle force can usually be obtained by using manual muscle testing (MMT), invasive direct measurement (IDM), and kinematic and dynamic method (KDM) [12]. However, these methods have many problems, such as high cost, low precision, and irreparable damage to the human body. In contrast, it is the most convenient, safest, and cheapest method to drive auxiliary training instruments and intelligent prosthetic devices by obtaining motion information from MMG. Therefore, MMG has been taken as an ideal non-invasive control signal.

The changes of MMG are closely related to muscle force, muscle fatigue, body posture, and movement [13–15]. Through the analysis and feature extraction of MMG, a recognition model can be built to recognize the movement patterns of limbs, but it is difficult to accurately estimate muscle force. Accurate muscle force estimation has great practical demand and extremely important application value in many fields [16–18]. However, there is no mature and stable technology to directly measure muscle force at present. The existing muscle force testing methods either need to use an external force measuring device to detect contact force, or the measuring conditions are too harsh to limit the application occasions. Therefore, it is a challenging problem to extract information from MMG to estimate muscle force accurately and timely. The muscle force accurately estimated by MMG can be used as the control input of the human-computer interaction system and can also monitor and feedback the health status and fatigue degree of human muscles in real-time, which is of great significance for intelligent artificial limbs and wearable devices.

At present, in addition to the successful use of sEMG signal to estimate human parameters [19–21], some experts and scholars have also begun to use MMG signal to construct estimation models for muscle force estimation. Studies have shown that there is a nonlinear relationship between MMG and muscle force [22], indicating that MMG can

be used to estimate muscle force. In order to effectively build the relationship between MMG and corresponding muscle force, Beck et al. [23] studied the linearity and reliability relationship between MMG amplitude and muscle force of vastus lateralis muscle and concluded that there was not enough linearity and reliability relationship between MMG amplitude and muscle force. Furthermore, they also pointed out that the relationship between MMG amplitude and muscle force could be improved by using new techniques. Further, Youn and Kim [24] extracted the MAV and the ZC of MMG as features and fed them into the artificial neural network (ANN). The feasibility of MMG for estimating the elbow flexion force was demonstrated. Then, by extracting the RMS and ZC of MMG as features, they confirmed that ANN models to estimate the elbow flexion forces are better than the multiple linear regression (MLR) models [25]. Although they were obtained satisfactory results, the accuracy was still not high. Therefore, they suggested using other learning techniques such as support vector machines to improve the model's accuracy in the future. Lei et al. [26] also adopted the same method to extract RMS and frequency-domain variance (FV) from MMG as features, and input them to the ANN for muscle force estimation, and concluded that the constructed regression model had higher accuracy than polynomial regression. However, the estimation accuracy of these models is not high enough. Although ANN is very popular in MMG muscle force estimation, it still has some drawbacks, such as easy convergence to a local optimal solution, poor generalization ability to produce overfitting results, empirical choice of hidden layer node number, random initialization of linkweights between network nodes, etc. Recently, to improve the accuracy of muscle force estimation, our research group tried to build an optimized relevance vector machine (RVM) to estimate the quadriceps femoris contraction strength by selecting MAV, MPF, SE, and the correlation coefficient between MMG signals in two different channels, but the effect of muscle force estimation was still not ideal.

Compared with ANN, radial basis function (RBF), and random forest (RF), support vector regression (SVR) is more suitable for complex and nonlinear regression problems based on statistical supervised learning theory and structural risk minimization. It has a perfect theoretical basis, strong fitting ability, strong generalization ability, and strong robustness [27]. Therefore, Zhang et al. [28] used SVM to classify head motion by extracting the time domain, time-frequency domain, and nonlinear dynamic features of MMG, achieving a suitable classification effect with an accuracy rate of 88.2%. In addition, some useful attempts have been made to estimate muscle force by using SVR. Ibitoye et al. [29] first used SVR to estimate the knee torque by selecting RMS and peak-to-peak (PP) values as MMG features. They obtained suitable estimation results with the coefficient of determination (R^2) of 89% and the root mean square errors (RMSE) of 12.95. Further, Wang et al. [30] selected the combination of four characteristics to estimate the knee joint extension force by using SVR, which obtained a suitable result with R^2 of 0.799 and RMSE of 9.18%. Ibitoye et al. [31] used SVR to estimate the neuromuscular electrical stimulation NMES evoked knee torque from MMG and obtained satisfactory results, with RMSE of range 6.28–9.82 and accuracy up to 95% by using Gaussian and polynomial support vector kernels.

In summary, it can be seen that SVR can be used for muscle force estimation. However, in parameter selection, SVR usually selects key parameters randomly, resulting in the model not obtaining high prediction accuracy. Consequently, we need to explore the optimal key parameter optimization method of SVR and build a muscle force estimation model. Although some algorithms have been proposed for SVR optimization and suitable results have been obtained, the need to develop new optimization algorithms will be increasing [32]. In this paper, we use the gray wolf algorithm (GWA) to optimize the penalty factor and kernel function parameter of SVR, but the traditional GWA is prone to premature, poor stability, easy to fall into local optimal [33]. To solve this problem, we introduce a new nonlinear convergence factor and a new position update strategy to improve the traditional GWA to balance local and global search capabilities.

The knee extension force is produced by an isolated extension, which mainly comes from four muscles of the quadriceps femoris in the front of the thigh. To accurately estimate knee joint extension force based on quadriceps muscle activity, an IGWO-SVR model is proposed, in which IGWO adopts a new nonlinear convergence factor and a new position update strategy. Compared with other estimation models, the IGWO-SVR model can obtain the best performance in different evaluation indexes. The main contributions of this study are as follows:

1. A new, improved swarm intelligence optimization algorithm (IGWO) combined with SVR is proposed. In the IGWO, a new nonlinear convergence factor and a new location update strategy are creatively proposed, which can effectively improve the estimation of knee joint extension force;
2. The new nonlinear convergence factor and the new position update strategy are applied to IGWO for the first time;
3. The first application of the proposed IGWO-SVR model in muscle force estimation;
4. The proposed IGWO-SVR model is superior to other models in performance indexes of RMSE, MAPE, and R.

2. Methodology

2.1. Support Vector Regression

Support vector machine (SVM) is a new type of supervised learning prediction method. Compared with some neural networks, this method has a reliable statistical theoretical basis and higher prediction accuracy for high-dimension and small-sample data and is especially suitable for nonlinear problems [34]. Its basic principle is to map low-dimensional feature vectors in the sample set to high-dimensional feature space through nonlinear transformation function (kernel function) and then perform linear regression fitting on the mapped sample set in the high-dimensional space. Thereby, it can transform the low-dimensional nonlinear regression problem into a high-dimensional linear one [35]. The principles of SVR are as follows.

Supposing a set of training samples, $S = \{(x_i, y_i) | (x_i \in R^n, y_i \in R)\}_{i=1}^L$, where x_i represents the input feature vector of the i th sample; y_i represents the actual value of the i th sample; n represents the dimension of input parameters; L represents the number of training samples. After mapping through a nonlinear function φ , the SVR function can be expressed as:

$$f(x_i) = w^T \varphi(x_i) + b \quad (1)$$

where $w \in R^n$ and $b \in R$ are the weight and bias vectors, respectively. w and b are estimated by the minimized regular risk function.

$$R(C) = C \frac{1}{L} \sum_{i=1}^L L_\varepsilon(y_i, f(x_i)) + \frac{1}{2} \|w\|^2 \quad (2)$$

where ε represents the maximum error allowed by the regression analysis, which is used to control the number of support vectors and generalization ability. C is a positive constant, also called the penalty factor, representing the degree of penalty for errors exceeding ε ; y_i and $f(x_i)$ are the actual value and predicted values of the i th sample, respectively. $L_\varepsilon(y_i, f(x_i))$ is ε -insensitive loss function to penalize the training errors between y_i and $f(x_i)$, and is defined as follows:

$$L_\varepsilon(y_i, f(x_i)) = \begin{cases} 0 & \text{if } |y_i - f(x_i)| < \varepsilon \\ |y_i - f(x_i)| - \varepsilon & \text{if other} \end{cases}, \varepsilon > 0 \quad (3)$$

The relaxation variables ξ and ξ^* are introduced, and the objective function is finally transformed as follows:

$$\min \frac{1}{2} \|w\|^2 + C \sum_{i=1}^L (\xi + \xi^*) \quad (4)$$

$$\text{s.t.} \begin{cases} y_i - f(x_i) \leq \varepsilon + \xi_i \\ -y_i + f(x_i) \leq \varepsilon + \xi_i^* \quad i = 1, 2, \dots, L \\ \xi_i, \xi_i^* \geq 0 \end{cases} \quad (5)$$

The convex optimization problem of Equations (4) and (5) can be converted to solve their duality problem. Two new Lagrange multipliers α_i and α_i^* are added to the solution, and the mapping is carried out through the kernel function $K(x_i, x_j) = \varphi(x_i)^T \cdot \varphi(x_j)$. Finally, the SVR function is expressed as follows:

$$f(x) = \sum_{i=1}^L (\alpha_i - \alpha_i^*) K(x_i, x) + b, \quad 0 < \alpha_i, \alpha_i^* < C \quad (6)$$

In the process of solving, the selection of kernel function has a great influence on SVR. Because the radial basis function (RBF) kernel has strong nonlinear approximation ability and suitable generalization performance when other parameters are appropriately selected, RBF function is chosen as kernel function, which is defined as follows:

$$K(x_i, x_j) = \exp(-\gamma \|x_i - x_j\|^2) \quad (7)$$

where $\gamma = \frac{1}{2\sigma^2}$, σ^2 is the variance of the kernel function.

In SVR calculation, penalty parameter C and kernel function parameter γ are often randomly selected, which has a great effect on the prediction accuracy of the model [36]. In addition, the trial-and-error method is time-consuming and insufficiently accurate. Therefore, optimization algorithms, such as grid search (GS), particle swarm optimization (PSO), gray wolf optimization (GWO), and cuckoo search (CS), can be selected to help SVR find these parameters and avoid over-learning or under-learning caused by improper parameter selection.

2.2. Traditional Gray Wolf Algorithm and Its Improvement

2.2.1. Traditional Gray Wolf Algorithm

Mirjalili et al. [37] proposed a GWO algorithm in 2014, which has been widely used in the field of neural network optimization. GWO algorithm is a new heuristic swarm intelligence optimization algorithm to simulate the hunting behavior of gray wolf packs. The algorithm has the advantages of simple structure, rapid convergence, and few adjustable parameters, which leads to the encouraging application of the GWO in various fields. The GWO optimization process can be described as follows: firstly, the gray wolf population is randomly generated in the search space, and gray wolf packs are divided into α wolves, β wolves, and δ wolves according to the fitness of each wolf from high to low, and the remaining individuals are ω wolves. These four categories are used to simulate the leadership hierarchy. Then, α , β , and δ wolves are used to locate the prey and guide the other wolves to calculate the distance between themselves and the prey to encircle and hunt. Finally, through the self-evolution of gray wolf packs, the distance is gradually shortened to realize the hunting prey, and the optimal solution of the problem to be optimized is obtained. The GWO optimization process is realized through wolves' behaviors such as encircling prey and hunting [38].

When gray wolves find prey, they will quickly approach the prey and update the distance and the position of gray wolves. The mathematical expression of their behavior of encircling prey is as follows:

$$\vec{D} = \left| C \cdot \vec{X}_P(t) - \vec{X}(t) \right| \quad (8)$$

$$\vec{X}(t+1) = \vec{X}_P(t) - A \cdot \vec{D} \quad (9)$$

where t represents the current iteration number, \vec{D} is the distance between the wolves and the prey, $\vec{X}_P(t)$ represents the position vector of t generation prey, $\vec{X}(t)$ represents the

position vector of gray wolves in the t generation, A and C are coefficients vectors, which can be expressed as:

$$A = 2a \cdot r_1 - a \quad (10)$$

$$C = 2r_2 \quad (11)$$

$$a = 2 - 2 \times \frac{t}{t_{max}} \quad (12)$$

where t represents the number of iterations, t_{max} represents the maximum number of iterations. a is the linear convergence factor (LCF), which decreases linearly from 2 to 0 during iteration. r_1 and r_2 are random values in $[0, 1]$, respectively. The random C can avoid falling into the local optima and keep the encircling behavior random.

When gray wolves encircle their prey and begin hunting (optimization), α , β and δ wolves lead other wolves (ω) to update their position vectors according to their fitness, which can be expressed as follows:

$$\begin{aligned} \vec{D}_\alpha &= \left| C_1 \cdot \vec{X}_\alpha - \vec{X}(t) \right| \\ \vec{D}_\beta &= \left| C_2 \cdot \vec{X}_\beta - \vec{X}(t) \right| \\ \vec{D}_\delta &= \left| C_3 \cdot \vec{X}_\delta - \vec{X}(t) \right| \end{aligned} \quad (13)$$

$$\begin{aligned} \vec{X}_1 &= \vec{X}_\alpha - A_1 \cdot \vec{D}_\alpha \\ \vec{X}_2 &= \vec{X}_\beta - A_2 \cdot \vec{D}_\beta \\ \vec{X}_3 &= \vec{X}_\delta - A_3 \cdot \vec{D}_\delta \end{aligned} \quad (14)$$

$$\vec{X}(t+1) = \frac{\vec{X}_1 + \vec{X}_2 + \vec{X}_3}{3} \quad (15)$$

where \vec{D}_α , \vec{D}_β , and \vec{D}_δ represent the distance, respectively. \vec{X} , \vec{X}_2 , and \vec{X}_3 in turn represent the real-time update positions of α , β and δ wolves, and $\vec{X}(t+1)$ represents the updated optimal solution vector. The location update strategy is implemented by averaging method (LUS1).

2.2.2. Improved Gray Wolf Algorithm

In practical application, the GWO algorithm also has some disadvantages, such as premature, poor stability, and easy to fall into local optimization [39]. It can be seen from the GWO algorithm that the deviation and convergence of gray wolves depend on the convergence factor a , which is linearly decreasing. However, the convergence of intelligent algorithms is nonlinear, and the linear process does not accord with the actual convergence process. Secondly, ω wolves update position according to the position of the three leading wolves, which means that ω wolves need to comprehensively learn and consider the position information of the three leading wolves simultaneously. However, the three leading wolves are treated the same in the traditional GWO algorithm; that is, the LUS1 is used to update the position, which is completely inconsistent with the actual situation. To find the optimal solution, the position information of α , β , and δ wolves should be fully considered. The weight of different position information should be given to accelerate the convergence speed of the algorithm and improve the ability to avoid trapping into local optimal [40]. To make up for the shortcomings of the traditional GWO algorithm, this paper improves the traditional GWO algorithm from two aspects of the convergence factors a and position-dynamic weights of α , β , and δ wolves.

1. Nonlinear convergence factor control strategy (NCF)

The optimization of the swarm intelligence algorithm mainly depends on the coordination ability between global search and local search. Strong global search ability can ensure that the algorithm is not “premature”. Strong local search ability can ensure that the algorithm can accurately search the extreme value. Since the linear variation of the convergence factor of the traditional GWO algorithm cannot reflect the whole optimization process, a new NCF is proposed.

$$a = \cos\left(\pi \log\left(1 + \frac{(e - 1)t}{t_m}\right)\right) + 1 \tag{16}$$

where t is the current iteration number and t_m is the maximum iteration number. The nonlinear evolution process of convergence factor a with the number of iterations is shown in Figure 1. It is clear that the convergence factor a decreases nonlinearly from 2 to 0 with the iteration number. At the initial stage of evolution, the convergence factor a is reduced steadily to realize the smooth transition of algorithm optimization. In the intermediate stage of evolution, the attenuation degree of convergence factor a increases, and the algorithm quickly finds the global optimal solution. In the later stage of evolution, the attenuation degree of convergence factor a gradually decreases, which ensures the precise optimization and final convergence of the algorithm. To prove the effectiveness of the proposed NCF, the proposed NCF is compared with LCF, and the results are shown in Table 1.

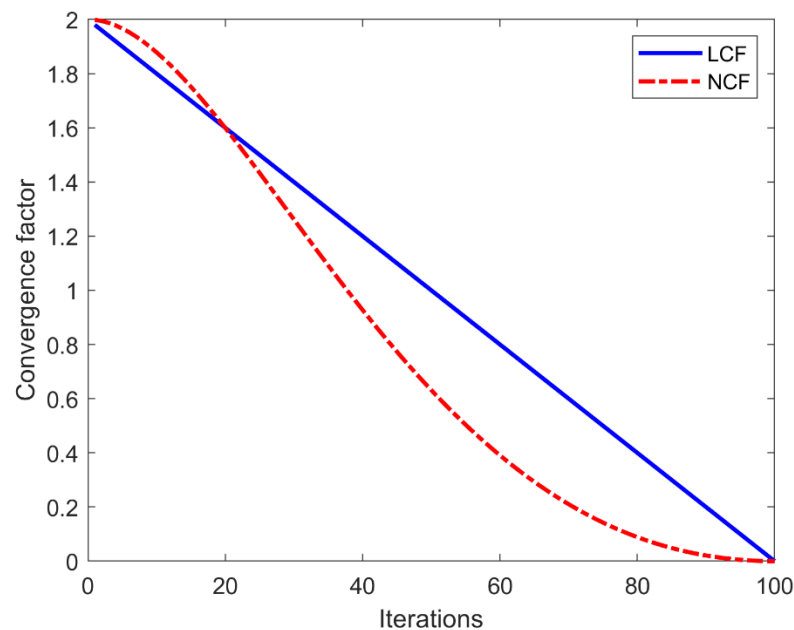


Figure 1. The comparison of two convergence factors.

Table 1. Comparison of different improvement strategies on the test samples of S1 subject.

	LUS1			LUS2		
	RMSE	MAPE	R	RMSE	MAPE	R
LCF	0.2962	0.0277	0.9972	0.2165	0.0274	0.9979
NCF	0.2050	0.0265	0.9980	0.1938	0.0256	0.9983

From Table 1, it can be seen that NCF can effectively improve the estimation performance of knee joint extension force. Therefore, the proposed nonlinear convergence factor can effectively balance global search and local search.

2. Update location strategy

When wolves search for prey, location update strategy plays a very important role in improving the efficiency of the algorithm. In the iterative process, it is easy to fall into local optimum as ω wolves approach α , β and δ wolves. By evaluating the positions of α , β and δ wolves, literature [41] introduced dynamic proportional weights and a new position updating strategy, which can avoid the shortcomings of the traditional GWO algorithm and achieve accurate hunting prey. Combined with the process of gray wolves encircling prey and hunting, the distance between ω and α , β , and δ wolves are noted as important for facilitating real-time location updates. Therefore, we propose a new position updating strategy (LUS2) based on the distance.

$$\omega'_1 = \frac{\frac{1}{|\vec{D}_\alpha|}}{\frac{1}{|\vec{D}_\alpha|} + \frac{1}{|\vec{D}_\beta|} + \frac{1}{|\vec{D}_\delta|}} \quad (17)$$

$$\omega'_2 = \frac{\frac{1}{|\vec{D}_\beta|}}{\frac{1}{|\vec{D}_\alpha|} + \frac{1}{|\vec{D}_\beta|} + \frac{1}{|\vec{D}_\delta|}} \quad (18)$$

$$\omega'_3 = \frac{\frac{1}{|\vec{D}_\delta|}}{\frac{1}{|\vec{D}_\alpha|} + \frac{1}{|\vec{D}_\beta|} + \frac{1}{|\vec{D}_\delta|}} \quad (19)$$

$$\vec{X}(t+1) = \omega'_1 \vec{X}_1 + \omega'_2 \vec{X}_2 + \omega'_3 \vec{X}_3 \quad (20)$$

where ω'_1 , ω'_2 , and ω'_3 correspond to the learning weights of α , β , and δ wolves, respectively. As can be seen from Table 1, the proposed LUS2 is superior to the traditional average location update strategy. Therefore, the proposed dynamic learning weight position update strategy can be better adjusted according to the actual situation and adapt to the new environment.

2.3. IGWO-SVR Model Construction

In the SVR model, the selection of penalty factor C and kernel function parameter γ directly affects the prediction and fitting effect of SVR. To further improve the accuracy of the model, we combine the IGWO algorithm with SVR and propose an IGWO-SVR estimation model. The specific implementation steps of the IGWO-SVR model are given below:

- (1) The experimental data are divided into training samples and test samples. If the quantity level difference between data is too large, the estimation result of SVR will be adversely affected. In addition, SVR is very sensitive to data between $[0, 1]$. To improve efficiency, the experimental data are normalized to the range $[0, 1]$, and the normalized equation is defined as follows:

$$x_{new} = \frac{x_i - x_{min}}{x_{max} - x_{min}} \quad (21)$$

where x_{new} represents the normalized data of each row, x_i represents each original input data, x_{min} and x_{max} represent the minimum and maximum values of each row data, respectively;

- (2) Set related parameters such as group size N , the maximum number of iterations t_m , and optimization parameter value range;
- (3) Initialize population randomly;

- (4) The fitness value of each wolf position is calculated and ranked in ascending order. The three leading wolves positions are denoted as \vec{X}_α , \vec{X}_β , and \vec{X}_δ , respectively. The fitness value in this paper is expressed by mean square error (MSE);
- (5) The distances are calculated according to (13) by updating the nonlinear convergence factor a . Then the new individual position $\vec{X}(t+1)$ is obtained according to (20); that is, the new SVR parameter values are obtained;
- (6) If the number of iterations reaches the maximum, the iteration is terminated, and the optimal parameters C and γ are output; Otherwise, return to (3) and continue the iteration;
- (7) The optimized parameters C and γ are used to establish the SVR estimation model.

2.4. IGWO-SVR for Knee Joint Extension Force Estimation

In this paper, by optimizing the key parameters of SVR with IGWO, a muscle force estimation model was constructed to realize the mapping of MMG features to knee joint extension force. Figure 2 shows the specific process of knee joint extension force estimation based on the proposed model. The process can be divided into three parts: signal acquisition and processing part, knee joint extension force estimation part, and result evaluation part.

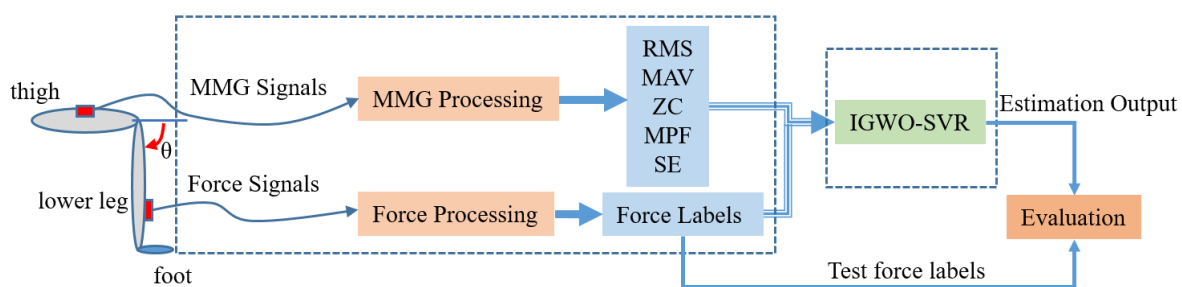


Figure 2. The specific process of knee joint extension force estimation based on IGWO-SVR and MMG.

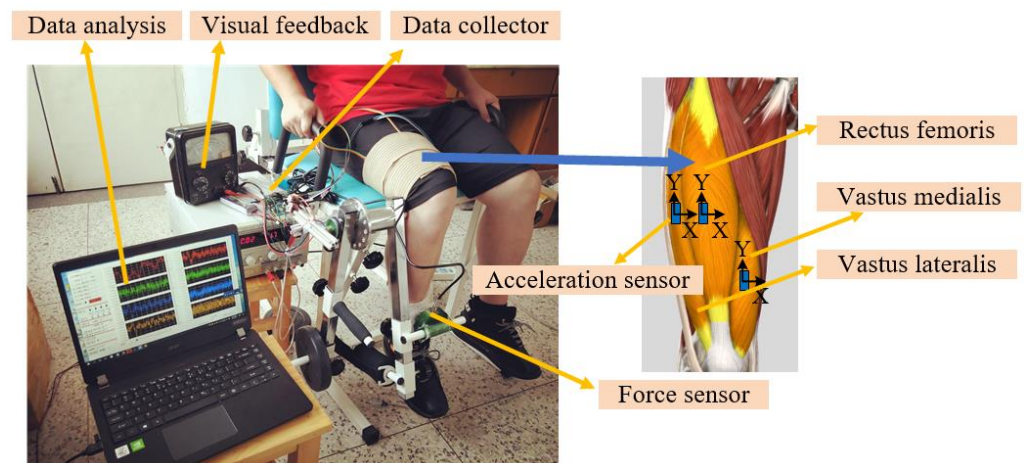
3. Experimental

3.1. Signal Acquisition and Processing

Four healthy male subjects (without neuromuscular and musculoskeletal diseases) were selected to participate in the experiment for data collection. The anthropometric data of the subjects are shown in Table 2. The experimental device and the acceleration sensor location are shown in Figure 3. The subjects were asked to sit comfortably in a test chair with their right leg fixed. A force sensor (DYL30, 0-300N, Bengbu Sensor, Inc., Bengbu, China) was placed in the front of the lower leg to measure the knee joint extension force. Acceleration sensors (ADXL335, ADI, Inc., Wilmington, MA, USA) and portable data collectors (VK702, VKinging, Inc., Shenzhen, China) are used to acquire MMG at a sampling frequency of 1000 Hz. Three acceleration sensors were bound to the clothes above the muscle belly of the rectus femoris (RF), vastus lateralis (VL), and vastus medialis (VM) by elastic bandages, respectively [30]. The subjects were required not to participate in any form of vigorous exercise within 48 h before the experiment, and were informed of the experiment procedure by the experimenter, and signed the informed consent form. This experimental scheme was approved by the Institutional Review Committee of Hefei Institute of Physical Science, Chinese Academy of Sciences. The data were collected twice. For the first time, subjects were familiar with the experiment process, and the maximum voluntary contraction force (MVC) of subjects was collected. For the second time, different strength forces and corresponding MMG were collected at 10~100% MVC with increments of 10% each time. Subjects were required to rest for 2~5 min at a time to avoid muscle fatigue while adjacent force level data were collected.

Table 2. Anthropometric data.

Subject	Age (Years)	Height (m)	Body Weight (kg)	Joint Angle (°)
S1	42	1.74	72.6	0~90
S2	29	1.70	68.0	0~90
S3	21	1.70	68.5	0~90
S4	21	1.72	66.5	0~90

**Figure 3.** Experimental setup and the acceleration sensor location.

Due to the low signal-to-noise ratio of the raw MMG signals, the raw MMG signals cannot be used directly. Therefore, it must be de-noised before further application. The power spectrum of MMG is mainly concentrated between 5 and 100 Hz, and the knee joint extension force signal is distributed below 2 Hz. Thus, a 5–100 Hz fourth-order Butterworth band-pass filter and a 2 Hz third-order Butterworth low-pass filter are applied to raw MMG signals and the corresponding extension force signal, respectively. The signals after primary de-noising are obtained, as shown in Figure 4. To obtain better data, 6 s stable extension force data are selected as experimental data. For the selected signals, the feature extraction is carried out by a sliding window with a window size of 1000 data points and a sliding step size of 100 data points. The MMG collected from muscles contains a large amount of force generation mechanisms information: the recruitment and the firing rates of motor units (MUs) [24], which are closely related to muscle force. To characterize MMG, RMS, MAV, ZC, MPF, and SE are selected as the features of MMG.

3.2. Model Evaluation Index

To evaluate the performance of the proposed model and other models, root mean square error (RMSE), mean absolute percentage error (MAPE), and correlation coefficient (R) are used to assess the accuracy of the knee joint extension force estimation. RMSE can measure the deviation between the estimated value and the actual value and is sensitive to outliers in the data. The smaller the value, the higher the accuracy of the estimation model. MAPE not only considers the error between the estimated value and the actual value but also considers the proportion between the error and the actual value, which can avoid the error canceling each other and accurately reflect the size of the actual estimation error. R reflects the overall deviation of the estimated value from the actual value. The closer R is to 1, the closer the estimated value is to the actual value. The equation of RMSE, MAPE, and R can be described as follows:

$$\text{RMSE} = \sqrt{\frac{1}{N} \sum_{i=1}^N (\hat{y}_i - y_i)^2} \quad (22)$$

$$\text{MAPE} = \frac{1}{N} \sum_{i=1}^N \left| \frac{\hat{y}_i - y_i}{y_i} \right| \quad (23)$$

$$R = \frac{\text{Cov}(\hat{y}_i, y_i)}{\sqrt{D(\hat{y}_i)}\sqrt{D(y_i)}} \quad (24)$$

where \hat{y}_i denotes the estimated value, y_i denotes the actual value, $D(\cdot)$ denotes the calculated variance, $\text{Cov}(\cdot)$ denotes the covariance, and N denotes the number of samples in the test set.

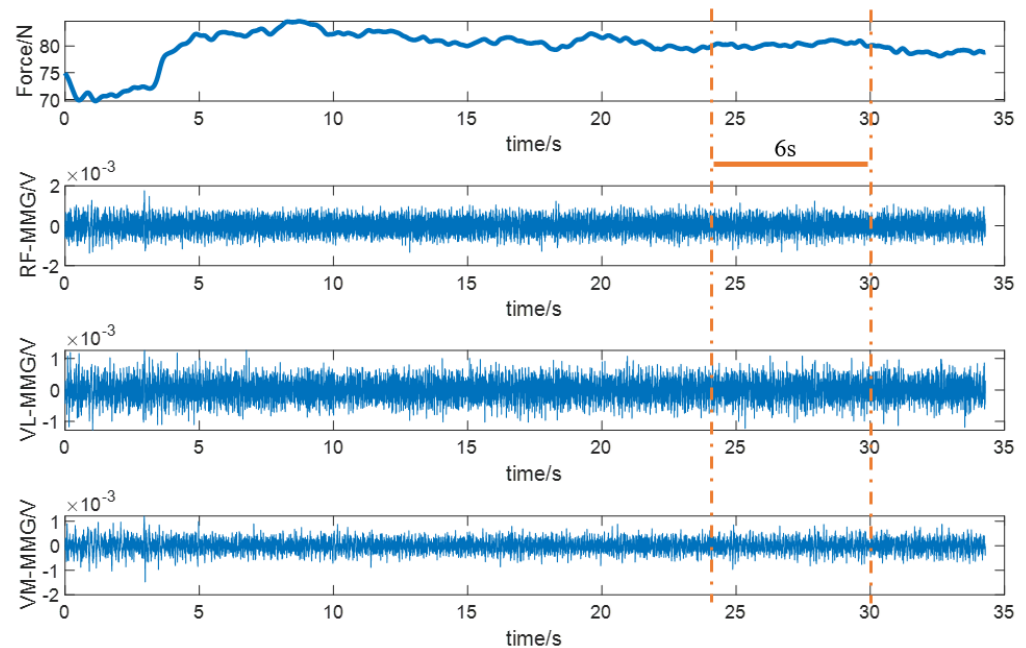


Figure 4. Signal and data selection after preprocessing.

3.3. Results and Discussion

The features of 3-channel MMG (RF-MMG, VL-MMG, and VM-MMG) under 10 different strength forces are extracted. Then, these features are combined to obtain a data set of 500 samples. Further, all the samples are scrambled, and the scrambled data are divided into the training set and test set, accounting for 90% and 10%, respectively. To verify the accuracy and effectiveness of the IGWO-SVR model in estimating knee joint extension force by MMG, in this paper, in addition to the comparison with back propagation neural network (BPNN), we also made a comparative analysis with RBF, generalized regression neural network (GRNN), SVR, GS-SVR, PSO-SVR, and GWO-SVR. The network structure of the BPNN model is 15-10-1, the number of iterations is 1000, the learning rate is 0.1, and other defaults. The expansion speed of RBF and the smooth factor of GRNN are both 0.4. The population and maximum iteration number of GWO are the same as those of PSO, which are 30 and 200, respectively. The optimization parameter range of GS, PSO, and GWO parameters is [0.01, 100].

Table 3 shows the estimated performance of different estimation models for subject S1. By comparing RMSE, MAPE, and R indexes, we find that the IGWO-SVR model is better than other models in estimating knee joint extension force, in terms of RMSE of 0.1938, MAPE of 0.0256, and R of 0.9983, respectively.

Figure 5 shows the estimation effects of knee joint extension force on S1 under different regression models. According to the fitting effects of estimated values and observed values in Figure 5a,b, it can be seen that the IGWO-SVR has the highest goodness of fit. Figure 5c shows the estimated results of the IGWO-SVR model for the test set, which clearly shows that the estimated values are basically in agreement with the observed values. It can be

concluded that the IGWO-SVR model is feasible and effective in the estimation of knee joint extension force.

Table 3. RMSE, MAPE, and R mean results for subject S1 under different regression models at the joint angle of 90.

Models	Evaluation Index			Models	Evaluation Index		
	RMSE	MAPE	R		RMSE	MAPE	R
BPNN	1.1841	0.0463	0.9958	GS-SVR	0.6712	0.1347	0.9842
RBF	1.5942	0.0389	0.9917	PSO-SVR	0.2817	0.0569	0.9883
GRNN	0.3278	0.1037	0.9849	GWO-SVR	0.2868	0.0748	0.9883
SVR	0.4006	0.1744	0.9715	IGWO-SVR	0.1938	0.0256	0.9983

In order to further verify the effectiveness and accuracy of the proposed IGWO-SVR in this paper, the estimation of knee joint extension force for four subjects is presented under different regression models, as shown in Figure 6. Figure 6a shows the RMSE comparison of four subjects under different estimation models. As can be seen from Figure 6a, the RMSE of IGWO-SVR is the smallest among all estimation models for four subjects; besides that, the PSO-SVR also obtained satisfactory results overall. As can be seen from Figure 6b, the MAPE of IGWO-SVR is the smallest among all the estimation models for the four subjects, except that GRNN, SVR, and GS-SVR generally performed the least satisfactory. As can be seen from Figure 6c, the R of IGWO-SVR is the largest among all the estimation models for the four subjects. In addition, SVR, GS-SVR, PSO-SVR, GWO-SVR, and IGWO-SVR overall show the sequentially improved performance of the evaluation R index. It can be clearly seen from Figure 6 that all indexes of IGWO-SVR are better than other regression models, i.e., the RMSE and the MAPE are the smallest, and the R is the largest among the four subjects. Further, the IGWO-SVR model has a strong generalization ability in estimating knee joint extension force for different subjects.

The mean results of RMSE, MAPE, and R are 0.2492, 0.0509, and 0.9967, respectively, for four subjects, as shown in Table 4. The IGWO-SVR model outperforms the other models in comparing classical neural network and optimized SVR models since the IGWO optimizer that was used has the highest optimization power.

Table 4. Mean results of RMSE, MAPE, and R for four subjects under different regression models at the joint angle of 90.

Models	Evaluation Index			Models	Evaluation Index		
	RMSE	MAPE	R		RMSE	MAPE	R
BPNN	0.9233	0.068	0.9948	GS-SVR	0.9346	0.1549	0.9801
RBF	1.3367	0.0859	0.9828	PSO-SVR	0.3738	0.0634	0.9871
GRNN	0.4854	0.1572	0.9782	GWO-SVR	0.4989	0.1183	0.9855
SVR	0.6194	0.2081	0.9701	IGWO-SVR	0.2492	0.0509	0.9967

Furthermore, to verify the effectiveness of the proposed model from other relevant aspects, this paper verifies the muscle force estimation effects of various models for four subjects under different joint angles (30°, 60°, 90°). Figure 7 shows the mean results of RMSE, MAPE, and R of four subjects at different angles. It can be obviously known that: (1) Although there are some differences between individuals, the proposed model achieves the best results, with the lowest RMSE, the lowest MAPE, and the highest R, compared with other models. (2) When the angle is at 90°, the estimation performance of all models is generally best in different angles. The reason is that the measured muscle is least interfered with by other muscles; that is, the quadriceps femoris can effectively represent the variation of knee joint extension force.

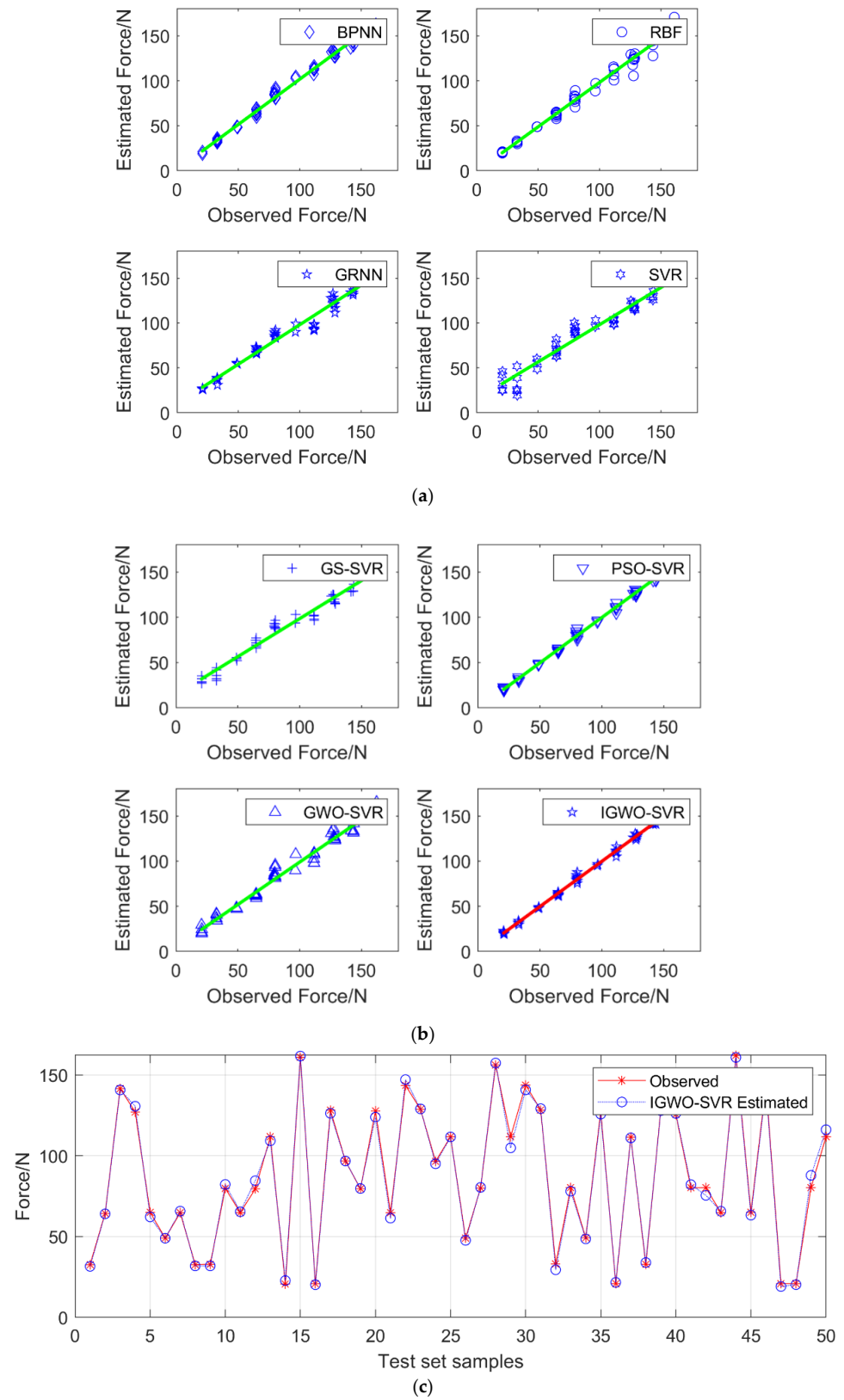


Figure 5. The estimation effects of knee joint extension force on S1 with different regression models at the joint angle of 90. (a) The fitting effects by BPNN, RBF, GRNN, and SVR. (b) The fitting effects by GS-SVR, PSO-SVR, GWO-SVR, and IGWO-SVR. (c) The estimated results of the IGWO-SVR model for the test set.

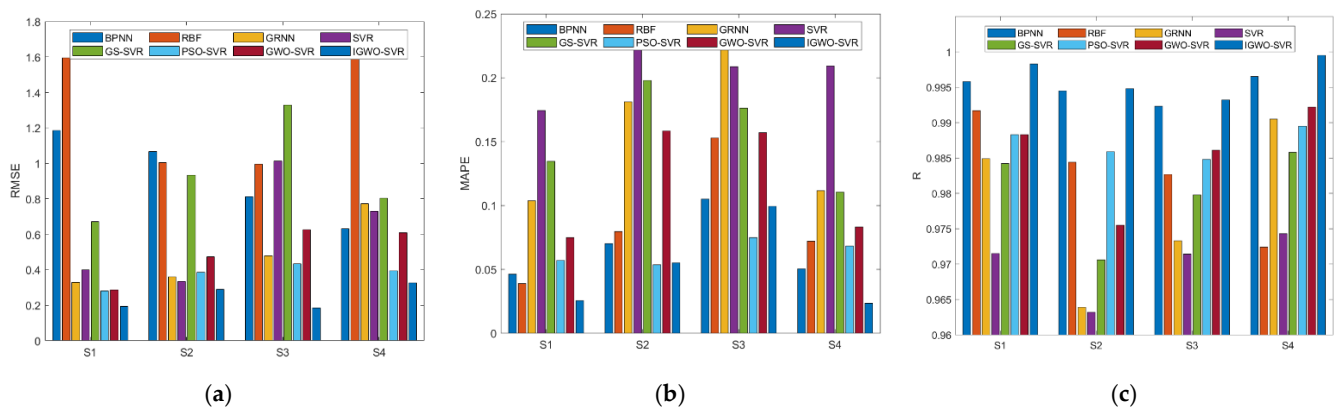


Figure 6. The estimation effect comparison of four subjects under different estimation regression models at the joint angle of 90. (a) The comparison of the RMSE index. (b) The comparison of the MAPE index. (c) The comparison of the R index.

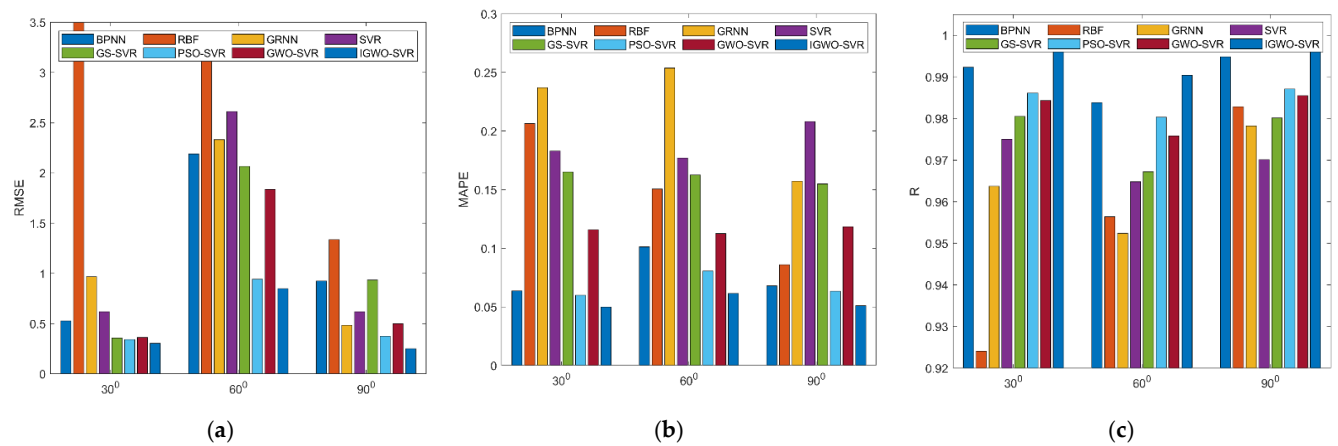


Figure 7. The comparative effects of estimation models for four subjects under different joint angles. (a) Mean results of RMSE index. (b) Mean results of MAPE index. (c) Mean results of R index.

In general, the estimated values obtained by the proposed model can fit the actual values well, and the evaluation indexes are highly acceptable as compared to the other current methods, which proves the effectiveness of IGWO-SVR estimation based on MMG features. In addition, the results estimated by other methods are also worth noting. Interestingly, it can be seen from Figures 6 and 7 that the optimized SVR model is generally superior to the neural network model in estimation performance because SVR improves the generalization ability of learning machines through minimizing empirical risk and structural risk and is more suitable for complex and nonlinear regression problems. Another interesting fact is that PSO-SVR generally outperforms GWO-SVR and GS-SVR in estimating knee joint extension force. Specifically, there are two reasons. One is that various agents in PSO can better adapt to the environment through mutual cooperation and improve the robustness of the algorithm. The other is that GS search in parameter space is affected by the search step size. In particular, when the step size is large, the search efficiency is improved, but the parameter optimization effect is poor. Moreover, GWO uses the traditional linear convergence factor and position average update strategy, which limit GWO’s excellent optimal searching ability. Meanwhile, compared with PSO, GWO has a simple structure, rapid convergence, and few adjustable parameters. Therefore, in view of the disadvantages of traditional GWO, this paper creatively designs nonlinear convergence factor and dynamic position update strategy, which can not only accelerate the fast convergence of the algorithm but also greatly improve the ability of parameter optimization and further improve the adaptability of the algorithm to MMG features. It can be shown again that the proposed IGWO-SVR model can be more accurate to deal with the actual MMG features

compared with other regression models and is very suitable for the estimation of knee joint extension force.

During the experiment, we also found that muscle tremor was severe when the subjects' muscle force was between 70% and 100% MVC. This may affect the temporal and spectral anomaly responses of the MMG during the force, which may also lead to a bias in the estimation of high muscle strength grades. In contrast, the muscle tremor is more stable and persistent when the subjects' muscle force is between 10% and 70% MVC. In this case, MMG may better reflect the recruitment and the firing rates of MUs, which also enables the estimation model to estimate muscle force more accurately.

4. Application and Limitation

The results of knee joint extension force estimation could provide more effective guidance information for the control of human joint auxiliary equipment. The flow chart is shown in Figure 8. As can be seen from the figure, an accurate force estimation model is a crucial factor in controlling human joint auxiliary equipment. Without a force estimation model that provides real-time muscle force information, the device guided by the motion intention-recognition module will be very stiff. In the future, the proposed model, which can accurately estimate the knee joint extension force, combined with the motion intention-recognition module, can realize the flexible control of human joint auxiliary equipment perfectly.

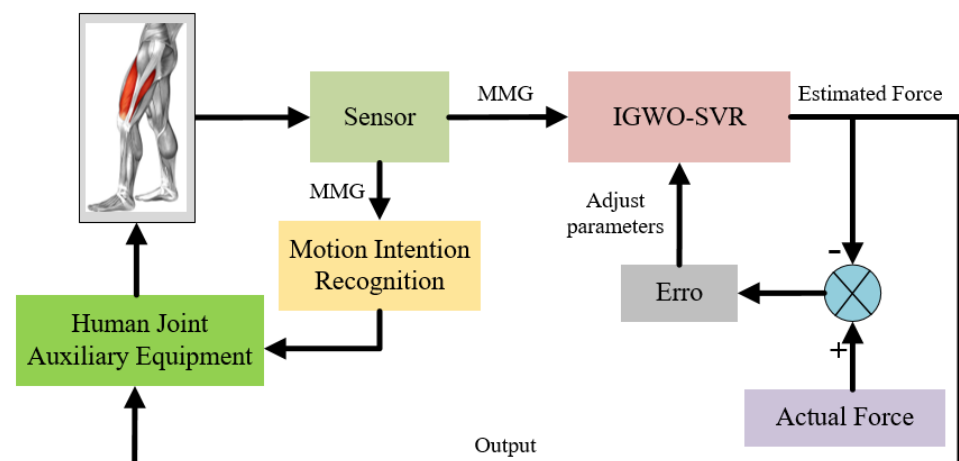


Figure 8. The application example of IGWO-SVR in human joint auxiliary equipment. Based on the recognition of motion intention and the knee joint extension force estimation, they can be used as effective input signals of the human joint auxiliary equipment to realize the compliant control of lower limb movement.

We designed the MMG-Force estimation model, which can be applied in the estimation of knee joint extension force under the condition of fixed knee joint angle, that is, the isolated movement. Hence, this study is limited to isometric quadriceps contraction and has some limitations, such as various muscle contractions and various muscle contributions, which may result in the failure of the model in lower limb flexion and extension movement such as walking and running. Therefore, future studies need to further consider the role of a wide range of possible factors in muscle activity.

5. Conclusions and Future Outlook

Since knee joint extension force can affect the reliability and comfort of lower limb assisted rehabilitation devices and intelligent prosthetic devices, it is necessary to establish an extension force estimation model based on MMG. In order to further improve the accuracy of the SVR model, the proposed IGWO algorithm in this paper was used to optimize the key parameters of SVR to achieve the accuracy of knee joint extension force

estimation. In the IGWO, a new nonlinear convergence factor and a new dynamic location update strategy were creatively proposed, which effectively balance global and local search capabilities. The proposed IGWO-SVR model was applied to estimate the knee joint extension force. Compared with BPNN, RBF, GRNN, SVM, GS-SVR, PSO-SVR, and GWO-SVR, the best performance indexes in terms of MSE, MAPE, and R were achieved. These results suggest that using the IGWO-SVR model may be a more reliable method to establish the complex, nonlinear relationship between the MMG and the corresponding force than the other models. It also further indicates that the proposed model can be applied to human joint auxiliary equipment to improve the flexibility and reliability of joint control.

Even though positive results have been achieved, some other works must be carried out further in the future.

- (1) In consideration of the influence of other lower limb motion parameters, such as motion angular velocity and body posture, on the estimation of lower limb muscle force;
- (2) Consider other improved swarm intelligence algorithms to optimize machine learning and further improve the accuracy of muscle force estimation;
- (3) Apply the estimation results to the recognition of human lower limb motion intention and the compliant control of the intelligent portable wearable robot.

Author Contributions: Conceptualization, L.G. and D.W.; methodology, Z.L.; software, Z.L.; validation, W.L., L.G. and D.W.; investigation, L.G., C.X. and H.C.; writing—original draft preparation, Z.L.; writing—review and editing, Z.L. and D.W.; visualization, H.C.; supervision, L.G.; project administration, D.W.; funding acquisition, L.G., H.C. and Z.L. All authors have read and agreed to the published version of the manuscript.

Funding: This research was funded by the Strategic Priority Research Program of the Chinese Academy of Sciences, Grant No. XDA22040303. Key scientific research projects of Anhui Province higher education, Grant No. KJ2020A0630. Teaching research projects of Anhui Province, Grant No. 2019jyxm0361. Key research projects supported by the National Natural Science Foundation of China, Grant No. 92067205. Supported by the HFIPS Director's Fund, Grant No. YZJJ2021QN25.

Institutional Review Board Statement: Ethical review and approval were approved by the Institutional Review Committee of Hefei Institute of Physical Science, Chinese Academy of Sciences. The approval number is no. SWYX-Y-2021-75. All subjects are composed of students and staff of the research group; no patients are involved. Moreover, there is no harm to the body in our experiment.

Informed Consent Statement: Informed consent was obtained from all subjects involved in the study.

Data Availability Statement: The data used to support the findings of this study are included within the article.

Acknowledgments: This work was partly carried out at the Robotic Sensors and Human-Computer Interaction Laboratory, Hefei Institute of Intelligent Machinery, Chinese Academy of Sciences.

Conflicts of Interest: The authors declare no conflict of interest.

References

1. Rathor, R.; Singh, A.K.; Choudhary, H.; Goswami, C.; Fekete, G. A systematic review on gait analysis methods and assistive devices in lower limb prosthetics. *Mater. Today Proc.* **2021**, *44*, 4251–4255. [[CrossRef](#)]
2. Ashghabadi, A.S.; Moqadam, S.B.; Xu, J. Multichannel finger pattern recognition using single-site mechanomyography. *IEEE Sens. J.* **2021**, *21*, 8184–8193. [[CrossRef](#)]
3. Jafarzadeh, M.; Hussey, D.C.; Tadesse, Y. Deep learning approach to control of prosthetic hands with electromyography signals. In Proceedings of the IEEE International Symposium on Measurement and Control in Robotics (ISMCR 2019), Houston, TX, USA, 19–21 September 2019; pp. A1-4-1–A1-4-11.
4. Song, Y.; Du, Y.; Wu, X.; Chen, X.; Xie, P. A synchronous and multi-domain feature extraction method of EEG and sEMG in power-assist rehabilitation robot. In Proceedings of the IEEE International Conference on Robotics and Automation (ICRA 2014), Hong Kong, China, 31 May–7 June 2014; pp. 4940–4945.
5. Na, Y.; Choi, C.; Lee, H.; Kim, J. A study on estimation of joint force through isometric index finger abduction with the help of semg peaks for biomedical applications. *IEEE Trans. Cybern.* **2016**, *46*, 2–8. [[CrossRef](#)]
6. Liang, X.; Wang, W.; Hou, Z.; Ren, S.; Peng, L.; Hu, J. Interactive control methods for rehabilitation robot. *Sci. Sin. Inf.* **2018**, *48*, 24–46. [[CrossRef](#)]

7. Vidovic, M.M.C.; Hwang, H.J.; Amsüss, S.; Hahne, J.M.; Farina, D.; Müller, K.R. Improving the robustness of myoelectric pattern recognition for upper limb prostheses by covariate shift adaptation. *IEEE T. Neur. Sys. Reh.* **2016**, *24*, 961–970. [[CrossRef](#)]
8. Oster, G.; Jaffe, J.S. Low frequency sounds from sustained contraction of human skeletal muscle. *Biophys. J.* **1980**, *30*, 119–127. [[CrossRef](#)]
9. Barry, D.T. Acoustic signals from frog skeletal muscle. *Biophys. J.* **1987**, *51*, 769–773. [[CrossRef](#)]
10. Posatskiy, A.O.; Chau, T. The effects of motion artifact on mechanomyography: A comparative study of microphones and accelerometers. *J. Electromyogr. Kinesiol.* **2012**, *22*, 320–324. [[CrossRef](#)] [[PubMed](#)]
11. Tarata, M.T. Mechanomyography versus Electromyography, in monitoring the muscular fatigue. *Biomed. Eng. Online* **2003**, *2*, 3. [[CrossRef](#)] [[PubMed](#)]
12. Wang, J.; Pang, M.; Yu, P. Effect of muscle fatigue on surface electromyography-based hand grasp force estimation. *Appl. Bionics. Biomech.* **2021**, *2021*, 8817480. [[CrossRef](#)]
13. Ibitoye, M.O.; Hamzaid, N.A.; Zuniga, J.M.; Wahab, A.K.A. Mechanomyography and muscle function assessment: A review of current state and prospects. *Clin. Biomech.* **2014**, *29*, 691–704. [[CrossRef](#)]
14. Naeem, J.; Hamzaid, N.A.; Islam, M.A.; Azman, A.W.; Bijak, M. Mechanomyography-based muscle fatigue detection during electrically elicited cycling in patients with spinal cord injury. *Med. Biol. Eng. Comput.* **2019**, *57*, 1199–1211. [[CrossRef](#)]
15. Cè, E.; Rampichini, S.; Limonta, E.; Esposito, F. Torque and mechanomyogram correlations during muscle relaxation: Effects of fatigue and time-course of recovery. *J. Electromyogr. Kinesiol.* **2013**, *23*, 1295–1303. [[CrossRef](#)]
16. Kasuya, M.; Seki, M.; Kawamura, K.; Fujie, M.G. Subtle grip force estimation from EMG and muscle stiffness—Relationship between muscle character frequency and grip force. In Proceedings of the Annual International Conference of the IEEE Engineering in Medicine and Biology Society (EMBC 2011), Boston, MA, USA, 30 August–3 September 2011; pp. 4116–4119.
17. Meng, W.; Ding, B.; Zhou, Z.; Liu, Q.; Ai, Q. An EMG-based force prediction and control approach for robot-assisted lower limb rehabilitation. In Proceedings of the IEEE International Conference on Systems, Man, and Cybernetics (SMC 2014), San Diego, CA, USA, 5–8 October 2014; pp. 2198–2203.
18. Anwar, T.; Jumaily, A.A. ANFIS to estimate damping coefficient from EMG to optimize the interaction force. In Proceedings of the International Conference on Microelectronics, Computing and Communications (MicroCom 2016), Durgapur, India, 23–25 January 2016; pp. 1–6.
19. Sepulveda, F.; Wells, D.M.; Vaughan, C.L. A neural network representation of electromyography and joint dynamics in human gait. *J. Biomech.* **1993**, *26*, 101–109. [[CrossRef](#)]
20. Li, Q.L.; Song, Y.; Hou, Z.G. Estimation of lower limb periodic motions from sEMG using least squares support vector regression. *Neural Process. Lett.* **2015**, *41*, 371–388. [[CrossRef](#)]
21. Wang, C.; Li, J.; Guo, C.; Huang, Q.; Yang, B.; Liu, H. sEMG-based estimation of human arm force using regression model. In Proceedings of the IEEE International Conference on Robotics and Biomimetics (ROBIO), Macau, China, 5–8 December 2017; pp. 1044–1049.
22. Akataki, K.; Mita, K.; Watakabe, M.; Itoh, K. Mechanomyogram and force relationship during voluntary isometric ramp contractions of the biceps brachii muscle. *Eur. J. Appl. Physiol.* **2001**, *84*, 19–25. [[CrossRef](#)] [[PubMed](#)]
23. Beck, T.W.; Defreitas, J.M.; Stock, M.S. The linearity and reliability of the mechanomyographic amplitude versus submaximal isometric force relationship. *Physiol. Meas.* **2009**, *30*, 1009–1016. [[CrossRef](#)] [[PubMed](#)]
24. Youn, W.; Kim, J. Estimation of elbow flexion force during isometric muscle contraction from mechanomyography and electromyography. *Med. Biol. Eng. Comput.* **2010**, *48*, 1149–1157. [[CrossRef](#)]
25. Youn, W.; Kim, J. Feasibility of using an artificial neural network model to estimate the elbow flexion force from mechanomyography. *J. Neurosci. Methods.* **2011**, *194*, 386–393. [[CrossRef](#)]
26. Lei, K.F.; Cheng, S.C.; Lee, M.Y.; Lin, W.Y. Measurement and estimation of muscle contraction strength using mechanomyography based on artificial neural network algorithm. *Biomed. Eng. Appl. Basis. Commun.* **2013**, *25*, 1350020. [[CrossRef](#)]
27. Zhang, X.; Tang, X.; Zhu, X.; Gao, X.; Chen, X.; Chen, X. A regression-based framework for quantitative assessment of muscle spasticity using combined EMG and inertial data from wearable sensors. *Front. Neurosci.* **2019**, *13*, 398. [[CrossRef](#)]
28. Zhang, Y.; Yu, J.; Xia, C.; Yang, K.; Cao, H.; Wu, Q. Research on GA-SVM based head-motion classification via mechanomyography feature analysis. *Sensors* **2019**, *19*, 1986. [[CrossRef](#)]
29. Ibitoye, M.O.; Hamzaid, N.A.; Wahab, A.K.A.; Hasnan, N.; Olatunji, S.O.; Davis, G.M. Estimation of electrically-evoked knee torque from mechanomyography using support vector regression. *Sensors* **2016**, *16*, 1115. [[CrossRef](#)]
30. Wang, D.; Xie, C.; Wu, H.; Hu, D.; Zhang, Q.; Gao, L. Estimation of knee extension force using mechanomyography signals detected through clothing. In *International Conference on Intelligent Robotics and Applications (ICIRA 2019)*; Springer: Cham, Switzerland, 2019; pp. 3–14.
31. Ibitoye, M.O.; Hamzaid, N.A.; Wahab, A.K.A.; Hasnan, N.; Olatunji, S.O.; Davis, G.M. SVR modelling of mechanomyographic signals predicts neuromuscular stimulation-evoked knee torque in paralyzed quadriceps muscles undergoing knee extension exercise. *Comput. Biol. Med.* **2020**, *117*, 103614. [[CrossRef](#)]
32. Huang, X.; Huang, X.; Wang, B.; Xie, Z. Fault diagnosis of transformer based on modified grey wolf optimization algorithm and support vector machine. *IEEE Trans. Electr. Electron. Eng.* **2020**, *15*, 409–417. [[CrossRef](#)]
33. Xie, Q.; Guo, Z.; Liu, D.; Chen, C.; Shen, Z.; Wang, X. Optimization of heliostat field distribution based on improved gray wolf optimization algorithm. *Renew. Energ.* **2021**, *176*, 447–458. [[CrossRef](#)]

34. Deris, A.M.; Zain, A.M.; Sallehuddin, R. A note of hybrid GR-SVM for prediction of surface roughness in abrasive water jet machining: A response. *Meccanica* **2017**, *52*, 1993–1994. [[CrossRef](#)]
35. Jiang, F.; Peng, Z.; He, J. Short-term load forecasting based on support vector regression with improved grey wolf optimizer. In Proceedings of the 10th International Conference on Advanced Computational Intelligence (ICACI 2018), Xiamen, China, 29–31 March 2018; pp. 807–812.
36. Zhou, Z.; Zhang, R.; Wang, Y.; Zhu, Z.; Zhang, J. Color difference classification based on optimization support vector machine of improved grey wolf algorithm. *Optik* **2018**, *170*, 17–29. [[CrossRef](#)]
37. Mirjalili, S.; Mirjalili, S.M.; Lewis, A. Grey wolf optimizer. *Adv. Eng. Softw.* **2014**, *69*, 46–61. [[CrossRef](#)]
38. Zhu, A.; Xu, C.; Li, Z.; Wu, J.; Liu, Z. Hybridizing grey wolf optimization with differential evolution for global optimization and test scheduling for 3D stacked SoC. *J. Syst. Eng. Electron.* **2015**, *26*, 317–328. [[CrossRef](#)]
39. Zhou, Y.; Yang, X.; Tao, L.; Li, Y. Transformer fault diagnosis model based on improved gray wolf optimizer and probabilistic neural network. *Energies* **2021**, *14*, 3029. [[CrossRef](#)]
40. Zhang, C.; Wang, W.; Pan, Y. Enhancing electronic nose performance by feature selection using an improved grey wolf optimization based algorithm. *Sensors* **2020**, *20*, 4065. [[CrossRef](#)] [[PubMed](#)]
41. Liu, Z.; Yang, B.; Ma, C.; Wang, S.; Yang, W. Thermal error modeling of gear hobbing machine based on IGWO-GRNN. *Int. J. Adv. Manuf. Technol.* **2020**, *106*, 5001–5016. [[CrossRef](#)]